Sensors and Actuators B 139 (2009) 13–21

Contents lists available at ScienceDirect

Sensors and Actuators B: Chemical

journal homepage: www.elsevier.com/locate/snb

Monitoring of enzymatic proteolysis on a electroluminescent-CCD microchip platform using quantum dot-peptide substrates

Kim E. Sapsford[a,*], Dorothy Farrell[b], Steven Sun[a,c], Avraham Rasooly[a,d], Hedi Mattoussi[b], Igor L. Medintz[e,**]

[a] Division of Biology, Office of Science and Engineering Laboratories, FDA, Silver Spring, MD 20993, USA
[b] Division of Optical Sciences Code 5611, U.S. Naval Research Laboratory, 4555 Overlook Avenue, S.W., Washington, DC 20375, USA
[c] Center for Advanced Sensor Technology, University of Maryland Baltimore County (UMBC), Baltimore, MD 21227, USA
[d] National Cancer Institute, Rockville, MD 20892, USA
[e] Center for Bio/Molecular Science and Engineering Code 6900, U.S. Naval Research Laboratory, 4555 Overlook Avenue, S.W., Washington, DC 20375, USA

ARTICLE INFO

Article history:
Available online 5 August 2008

Keywords:
Electroluminescent excitation
CCD
Resonance energy transfer
FRET
Quantum dots
Peptides
Protease sensor
Trypsin
Microfabricated device
Biosensor

ABSTRACT

Microfabricated devices will have a large impact on many aspects of analytical chemistry from clinical diagnostics to security applications due to their small size, ease of fabrication, portability and low sample volumes. In this report we compare quantum dot (QD)-peptide fluorescence resonance energy transfer (FRET) and subsequent FRET-based monitoring of enzymatic proteolysis on both a conventional laboratory fluorescent assay plate reader and an electroluminescent-charged-coupled device (EL-CCD) microchip detection platform. The EL-CCD setup combines the spatial detection of CCD with the simple illumination provided by EL strips to measure fluorescence from multi-well credit card-sized sample chips. Data on FRET between a QD donor and a dye-labeled peptide acceptor along with their usage as a substrate for trypsin proteolysis were collected on both platforms and analyzed. Despite a greater than 12-fold reduction in assay volumes in the microchip format and simplification of excitation/emission monitoring, the data reflected a general agreement including an analysis of the QD donor–dye acceptor FRET efficiency and the determination of proteolytic kinetic parameters such as enzymatic velocity V_{max} and the Michaelis constant K_M. The EL-CCD was further utilized to monitor specific ovomucoid inhibition of trypsin activity. The results suggest that the unique properties inherent to QDs can be combined with the reduced-scale nature of microfabricated devices to make them suitable for a variety of focused bioanalytical applications, including point-of-care diagnostics and global healthcare applications.

1. Introduction

The benefits of performing all forms of chemical analysis in a reduced scale on microfabricated devices are rapidly being realized [1–4]. The myriad applications that utilize these devices including point-of-care (POC) clinical diagnostics, global healthcare applications, pharmaceutical screening, and stand-alone security sensors will all benefit from their resulting scaled-down properties. These devices are portable, easy to fabricate and consume low sample volumes which can all reduce operational costs [1–4]. As the design and fabrication aspects mature, the focus shifts to the development and optimization of the assays performed on these devices [4–7]. Of particular importance are the choices of assay design, the signal transduction modality and the reagents utilized. It is clear that both simplification and wide applicability are key criteria to be incorporated [1–4].

The unique properties of luminescent semiconductor nanocrystals or quantum dots (QDs) suggest that they may be especially well-suited to broad utilization as a fluorescent label in microchip-based assays. Along with high quantum yields and exceptional resistance to both chemical- and photo-degradation, QDs possess narrow size-tunable photoluminescent (PL) emissions coupled to broad absorption spectra and high molar extinction coefficients. In addition, the ability to excite them at any wavelength below their emission band allows large effective Stoke's shifts [8,9]. QDs also have unique properties that make them ideal fluorescence resonance energy transfer (FRET) donors [10,11]. They can function as both an exciton donor and a central nanoscale platform for attaching multiple dye-acceptors, which proportionally increases the FRET efficiency [12]. A QD donor emission can be chosen such

* Corresponding author.
** Corresponding author. Fax: +1 202 767 9594.
E-mail addresses: Kim.sapsford@fda.hhs.gov (K.E. Sapsford), Igor.Medintz@nrl.navy.mil (I.L. Medintz).

0925-4005/$ – see front matter © 2008 Elsevier B.V. All rights reserved.
doi:10.1016/j.snb.2008.07.026

that it optimizes spectral overlap with a designated acceptor and the QD in this FRET pair can be excited at a wavelength that minimizes direct acceptor excitation; two particularly important FRET requirements [10–12]. QDs also offer the possibility of multiplex sensing based on immuno-fluorescence and FRET formats [13,14]. Cumulatively, these unique properties suggest that QDs can simplify the excitation and emission instrumentation needed to perform both fluorescent and FRET-based assays on microchip devices.

As a super-family of enzymes, proteases play key functions in many normal biological processes [15,16], are participants in many diseases including cancer along with several genetic disorders [15–18], and many infectious bacterial and viral microorganisms use proteases as essential virulence factors [15,19,20]. As such, monitoring proteolytic enzymes is directly important to pharmaceutical drug development, certain biowarfare agent detection and clinical diagnosis [5,16,21]. FRET-labeled peptide substrates have already been applied to detecting a number of proteases including botulinum neurotoxins [22], Hepatitis C virus protease [23], trypsin [24–26], and HIV protease [27]. In a previous report we described the use of specifically designed peptide substrates conjugated to QDs, where control over the average number of peptides attached per QD, allowed us to specifically monitor the activity of the proteases chymotrypsin, collagenase, caspase-1, and thrombin [28]. We further demonstrated the utility of this QD-peptide sensor conjugate by performing a pharmaceutical screening assay of potential thrombin inhibitors [28].

In this report, we demonstrate the use of an electroluminescent (EL)-charged-coupled device (CCD)-microchip platform for characterizing FRET-based QD-peptide bioconjugates as substrates for protease sensing and compare the results to the same assays carried out in a standard 96-well assay plate with a conventional fluorescent plate reader. Changes in FRET were monitored in response to trypsin addition, which cleaved the dye-labeled peptides and altered the FRET in a concentration-dependent manner (see schematic in Fig. 1A), and data were analyzed within the Michaelis–Menten kinetic model. Measurements in the presence of the trypsin inhibitor ovomucid were also carried out on the microchip. Despite an order of magnitude reduction in assay volumes and simplification of excitation/emission monitoring on the microchip, the data showed a remarkable equivalence across the two platforms, suggesting that QDs may indeed be ideal fluorophores for utilization on these devices.

2. Materials and methods

2.1. Materials

All chemicals were reagent grade and used as received from the manufacturer. *N*-[2-hydroxyethyl] piperazine-*N*′[2-ethane sulfonic acid] (HEPES), phosphate buffered saline (137 mM NaCl, 10 mM phosphate, 2.7 mM KCl, pH 7.4, PBS), imidazole, HPLC grade acetonitrile, Tween-20, Corning® 96-well white polystyrene non-binding surface (NBS™) plates, trypsin (from bovine pancreas, M_W ~24 kDa, 10,000 BAEE units/mg) and the trypsin inhibitor, ovomucoid, were obtained from Sigma–Aldrich (St. Louis, MO). The peptide sequence CSTRIDEANQRATKL$(P)_7S(H)_6$ was synthesized by EZBioLab custom peptide service (Westfield, IN). Nickel-nitroloacetic acid (Ni-NTA) agarose media was purchased from Qiagen (Valencia, CA). OPC oligonucleotide purification cartridges and triethylamine acetate buffer (TEAA) were obtained from Applied Biosystems (Foster City, CA). Cy3-maleimide mono-reactive dye was purchased from Amersham Biosciences (Piscataway, NJ).

2.2. QD synthesis

CdSe–ZnS core–shell QDs with emission maxima centered at 530 nm were synthesized using stepwise reactions of organometallic precursors in hot coordinating solvent mixtures following the procedures described in references [29–32]. The nanocrystals were made hydrophilic by exchanging the native capping shell of trioctyl phosphine and trioctyl phosphine oxide (TOP/TOPO) with bifunctional dihydrolipoic acid–poly(ethylene glycol)-ligands (DHLA–PEG_{600}, PEG $M_w \cong 600$), as described in references [33,34]. QD absorption and emission spectra and DHLA–PEG_{600} ligand structure are provided in Fig. 1B and C.

2.3. Fluorescent labeling of the peptide

1 mg peptide was initially dissolved in 1 mL of 10× PBS and the peptide solution then combined with Cy3-maleimide mono-reactive dye. The reaction mixture was incubated overnight at 4 °C and unreacted Cy3 dye was removed by purification with three consecutive 0.5 mL columns of Ni-NTA–agarose. After loading the reaction onto the Ni-NTA media, the columns were washed with 10 mL PBS before the Cy3-peptide was eluted with 300 mM imidazole in PBS. A reverse-phase OPC oligonucleotide purification

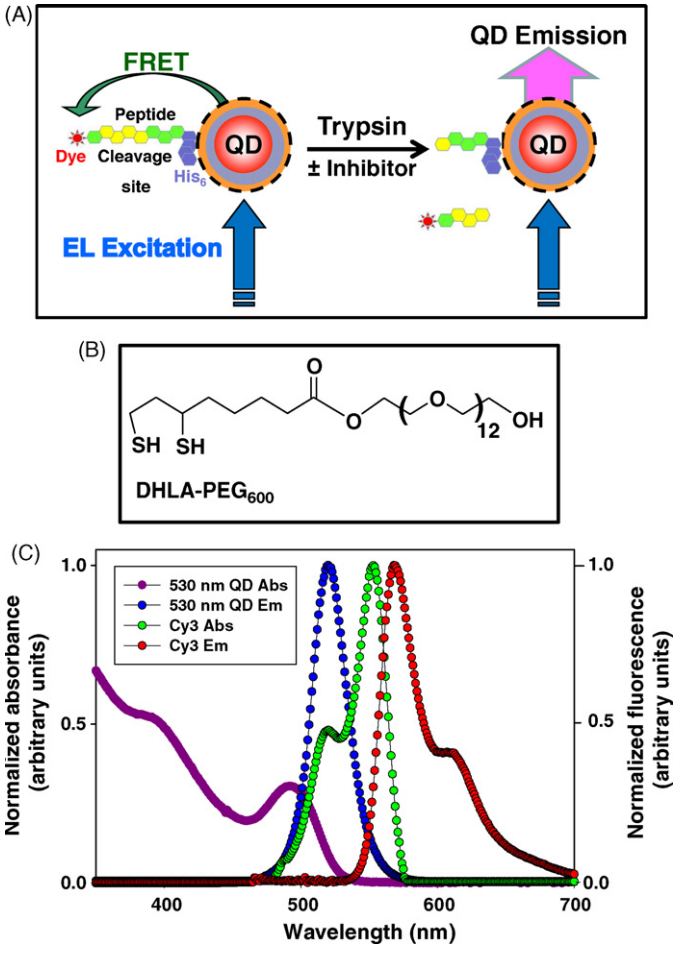

Fig. 1. QD-Cy3-peptide sensor construct and the optical characteristics of the utilized fluorophores. (A) Schematic diagram of the QD-Cy3-peptide FRET-based sensor constructs. Cy3 labeled peptides containing appropriate cleavage sites for trypsin are self-assembled onto the QD surface. FRET from the QD to the Cy3 dye quenches the QD PL. Trypsin cleaves the peptide altering the FRET signature. (B) DHLA–PEG_{600} chemical structure. (C) Normalized absorption and emission profiles of the 530 nm QDs and Cy3 dye used in this study.

cartridge was then used to remove the imidazole and desalt the Cy3-peptide. The OPC was first washed with 3 mL acetonitrile followed by 3 mL 2 M TEAA. The Cy3-peptide was loaded onto the column and washed with 50 mL 0.02 M TEAA and the desalted Cy3-peptide eluted, using 1 mL 70% acetonitrile in H_2O. The column was then regenerated by washing with 3 mL acetonitrile followed by 3 mL 2 M TEAA, and the remaining sample solution reloaded for further rounds of purification as needed. The desalted Cy3-peptide was characterized by UV–vis spectroscopy before being aliquoted, dried down and stored at −20 °C until required.

2.4. Fabrication of the 16-well sample chips

The 16-well sample chips used in this study were designed in CorelDraw11 (Corel Corp. Ontario, Canada) and then micromachined in 1/8 inch black poly(methyl methacrylate) (PMMA) (Total Plastics, Harrisburg, PA) using a computer controlled Epilog Legend CO2 65W laser cutter (Epilog, Golden, CO). Before cutting, both sides of the acrylic sheets were coated with 3 M 9770 adhesive transfer double sided tape (Piedmont Plastics, Beltsville, MD), which was later used to attach the polycarbonate (PC) tops and bottoms which were also cut using the laser cutter. The wells were cleaned using Versa Clean® (FisherBrand, Pittsburgh, PA), followed by washing with MilliQ water before drying with air, see Fig. 2.

2.5. Fluorescence detection

A schematic of the assembled microchip sensing platform developed at the FDA is shown in Fig. 2 and consists of a Royal Blue Electroluminescent (EL) strip (width 2.5 cm, length cut to the length of the chip ~7 cm) with a broad emission over the blue-green wavelength range (Being Seen Technologies, Bridgewater, MA), a blue bandpass excitation filter HQ480/20× (Chroma Technology Corp, Rockingham, VT), a green bandpass emission filter D535/40 m (Chroma Technology Corp Rockingham, VT), and a cooled CCD Atik 16 camera (Adirondack Video Astronomy, Hudson Falls, NY), equipped with a 5 mm Pentax extension and Pentax 12 mm f1.2 lens (Spytown, Utopia, NY: Model Number C61229). A number of Pentax CCTV manual focus lenses, of varying focal lengths, were investigated and the lens chosen (Model Number C61215)

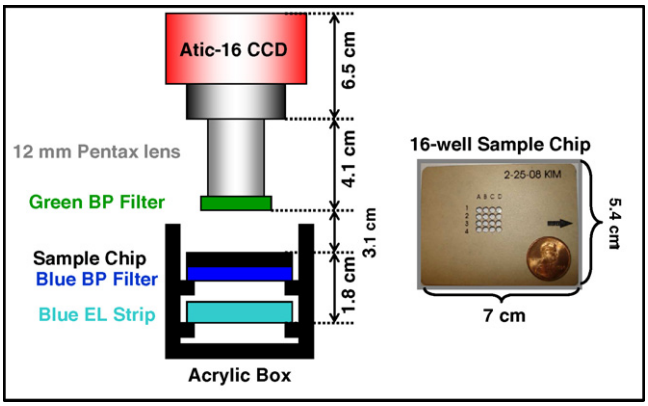

Fig. 2. Schematic configuration of the EL-CCD microchip platform designed by Rasooly and co-workers [42] (note, not to scale). The Atic-16 CCD camera is equipped with a 5 mm extension tube attached to a 12 mm Pentax f1.2 lens, pertinent dimensions are included. A green band pass emission filter is mounted on the end of the lens. The black acrylic box was designed to hold the blue EL strip, the blue band pass excitation filter and the acrylic 16-well sample chips, shown in more detail in the photograph (US penny coin included for scale). Sample chip dimensions of 5.4 cm by 7 cm fit the acrylic box platform that holds the EL excitation source and the blue excitation filter. The 16-sample wells are confined within a 1.2 cm × 1.2 cm square located in the optimal position for imaging.

was found to be optimal for the current configuration of the EL-CCD detector platform described. All the system components are enclosed in a black plastic box of dimensions 3 in. × 6 in. × 8 in. (Radioshack; www.radioshack.com). The EL requires 110 AC volts supplied by an inverter (Being Seen Technologies, Bridgewater, MA). The CCD was equipped with a 16-bit analog-to-digital converter allowing a dynamic range of 65,536 levels of grayscale to be discerned. For assays, the microchip's wells were filled with 7 μL/well and imaged with the EL-CCD platform using exposure times of 30 s and 60 s. The fluorescence images collected on the CCD were integrated and the intensities analyzed using ImageJ software (rsb.info.nih.gov/ij/download.html). The ImageJ software allows the mean intensity from the CCD image to be measured in areas defined by the user. As described previously [42], intensities from individual samples wells within the CCD image were analyzed using a circle that encompassed an area ~20% of the overall well area, allowing us to avoid the lighter circles that appear around the parameter of the well images, see later figures. Mean intensity measurements for all 16 wells in the CCD image were then imported into Microsoft Excel (Microsoft, Redmond, WA). The plate assays were conducted using standard 96-well plates and spectra were collected using a Tecan Safire Dual Monochromator Multifunction Plate Reader (Tecan, Research Triangle Park, NC), set to average 9 readings per well.

2.6. QD-peptide FRET and trypsin assays

QD-donor to Cy3-acceptor labeled peptide FRET efficiency was evaluated by self-assembling an increasing molar ratio of dye-labeled peptide per QD. This data was also used as a calibration curve for converting changes in FRET efficiency collected from the trypsin assay into enzymatic velocity (detailed below). The Cy3-peptide was resuspended by dissolving in DMSO (~5% of the final volume) followed by 20 mM HEPES + 0.1% Tween-20 pH 8. Samples consisted of 20 pmoles of the QD-DHLA–PEG_{600} mixed with Cy3-peptide at molar ratios of peptide-to-QD ranging from 0 to 10 in HEPES buffer. Final sample volumes utilized were 7 μL for the EL-CCD microchip studies and 100 μL for the plate reader studies. The solutions were incubated at room temperature for 30 min before use. Control experiments were carried out with free Cy3 alone and QD with free Cy3 to account for direct excitation of the dye and solution-based FRET interactions.

For the trypsin assay, an optimal QD:Cy3-peptide ratio of 1:2 was exposed to the indicated concentrations of trypsin or no enzyme control. Samples were mixed with enzyme and immediately loaded into the sample microchips or the 96-well plate for 5–10 min incubations and subsequent fluorescent measurement. Trypsin inhibition by ovomucoid was also monitored using the 16-well sample chips. The trypsin inhibition assay was preformed as described above with the addition of 1 μg of ovomucoid to each trypsin concentration point prior to the addition of the Cy3-peptide-QD. All assay points were performed in duplicate to triplicate and standard deviations are shown where appropriate.

2.7. Data analysis

Experimentally, the FRET efficiency E_n (n is the number of dye-acceptors per QD) was determined using:

$$E_n = \frac{(F_D - F_{DA})}{F_D} \quad (1)$$

where F_D and F_{DA} designate the fluorescence intensities of the donor alone and the donor in the presence of acceptor(s), respectively [35]. The data from FRET efficiency were then analyzed within the Förster formalism to determine values for center-to-center (QD-

to-dye) separation distance r using expression (2) developed for a centro-symmetric QD-peptide-dye conjugates [11,12]

$$r = \left(\frac{n(1-E_n)}{E}\right)^{1/6} R_0 \quad (2)$$

R_0 designates the Förster distance corresponding to $E_{n=1} = 0.5$ [35]. Because of the rather high FRET efficiencies measured for our set samples (compact conjugates), heterogeneity in the conjugate valence needed to be accounted for in the analysis, in particular for low ratios [28]. Using a Poisson distribution function, $p(k,n)$, to describe the heterogeneity in conjugate valence, the FRET efficiency E in Eq. (2) can be further written as [36]:

$$E(n) = \sum_{k=1}^{\infty} p(k,n)E(k) \text{ with } p(k,n) = \frac{e^{-n}n^k}{k!} \quad (3)$$

where n is the average acceptor-to-QD ratio used during reagent mixing and k the exact number of peptide-dye conjugated to the QD.

For the trypsin assays, changes in the FRET efficiencies following exposure of QD-substrate to increasing enzyme concentrations were compared to the FRET calibration curves, and a measure for the concentration of digested substrate was determined as detailed in reference [28]. Enzymatic velocities were then deduced by converting the amount of digested peptide P to a concentration of digested substrate per unit time ($d[P]/dt$). In the excess enzyme assay conditions used here, the maximum reaction rate V_{max} and the Michaelis constant K_M (the enzyme concentration at which the reaction proceeds at half the maximum rate) were then determined using:

$$V = \frac{d[P]}{dt} = \frac{V_{max}[E]}{K_M + [E]} \quad (4)$$

where $[E]$ is the enzyme concentration [37–40]. For assays carried out in the presence of ovomucoid a known competitive inhibitor of trypsin, the inhibition constant K_i was determined using:

$$K_M^{app} = K_M\left(1 + \left\{\frac{[I]}{K_i}\right\}\right) \quad (5)$$

where K_M^{app} is the apparent Michaelis constant in the presence of a competitive inhibitor [37–40].

3. Results and discussion

3.1. Peptide self-assembly and fluorescent monitoring

Upon assembling the peptide-dye onto the QD, FRET interactions cause significant quenching of the QD donor PL. Added protease cleaves the peptide freeing the acceptor dye from the surface of the QD donor resulting in concentration-dependent increase in QD donor PL, which is monitored for readout. The 530-nm QDs used in this study are made biocompatible through cap exchange of the native capping ligands with DHLA–PEG_{600} (see Fig. 1B and C). Similar to the design criteria outlined in our previous study [28], the peptide structure used here consists of three essential components; (1) the polyhistidine $(His)_6$ segment which attaches the peptide to the surface of the QD via self-assembly, (2) the enzyme cleavage site, and (3) a unique terminal cysteine-residue which is labeled with the Cy3 acceptor dye in this case. We have recently confirmed that formation of the QD conjugate is mediated by metal-affinity coordination interactions between the peptide's N-terminal $(His)_6$-tract and the metallic surface of the CdSe–ZnS core–shell QDs [41]. We demonstrated that these interactions are driven by a strong binding affinity with a derived dissociation constant of ~1–10 nM and provides for stable and functional conjugates within 10–15 min of reagent mixing [28,41].

In this study we characterize the FRET-based protease biosensor using both a standard laboratory 96-well Plate Reader and an EL-CCD microchip platform, schematically shown in Fig. 2. The EL-CCD microchip platform was designed with the aim of producing a portable, simple and inexpensive fluorescence detection system capable of measuring multiple samples simultaneously and was recently demonstrated using a commercial FRET-assay for botulinum neurotoxin A [42]. Within the fluorescent detector, minimal optics are required beyond a focusing lens coupled with a blue bandpass filter used to select a narrow excitation band and a green bandpass filter (placed after the sample) used to isolate the QD PL and discard the excitation signal from the final CCD image. The need for waveguides, line generators, and mirrors that typically accompany other optical-based detection systems are bypassed. The 16-well microchips require a rather small sample volume of ~7 μL. The number of available wells on the microchip can, and has been, easily scaled up to 96 during fabrication as desired. This setup contrasts with the Plate Reader which uses a complex excitation and multi-mirror/multi-lens/multi-PMT setup, and where assays require 100 μL sample volume [28].

3.2. Determination of FRET efficiency

We began by evaluating the FRET characteristics for the peptide-QD bioconjugates collected on both platforms. Fig. 3A shows the composite PL spectra for increasing molar ratio of peptide-dye-to-QD collected on the Plate Reader (excitation at 300 nm). Fig. 3B shows the corresponding loss in QD PL (converted to percentage of the initial value) along with the FRET efficiency E. Fig. 3C and D, respectively, show a typical fluorescence image for the same sample ratios collected on the EL-CCD microchip setup and the corresponding FRET efficiencies. Also shown within each figure is the QD PL loss as a function of the Cy3-peptide:QD ratio (plotted as percentage of the initial value). Clearly, the QD PL decrease traces the ratio of Cy3-peptide-to-QD used for either set of data. On the EL-CCD microchip, the donor PL decrease can be easily detected from the fluorescence image before integration and analysis, an indication that the emission filter allowed effective selection of the QD PL with minimal contribution from the dye. Control experiments on the standard plate reader using solutions of QDs mixed with free dye or dye-alone showed that solution-phase FRET and direct excitation contribution to dye emission were very small (data not shown). Similarly, control experiments on the EL-CCD microchip platform using solutions of QDs mixed with free Cy3 dye showed a QD PL loss due to solution-phase FRET much smaller than those measured for Cy3-peptide conjugates. Cy3 dye only controls showed that leakage of the acceptor emission into the QD channel as well as direct excitation contribution to the Cy3 emission are negligible (see supplementary data Figure S1).

This set of data proves that changes in the PL spectra result from FRET interactions between QD and dye. In both cases, rather large FRET efficiencies were measured, though the values extracted from the microchip were slightly higher. For instance, at an average ratio of one peptide per QD ~70% QD quenching is measured for the plate assay and ~80% is measured on the microchip. For this reason, only the plots for peptide-Cy3-to-QD ratios ranging between 0 and 4 are included; E essentially saturates at higher values. Fits to the data, carried out within the Förster formalism combined with the Poisson distribution to account for conjugate heterogeneity using Eqs. (2) and (3), are shown in Fig. 3B and D. The experimental values for the FRET efficiencies collected on both systems were higher than those predicted for ratios between 0 and 2, even though the difference between experiment and fit is less pronounced for data

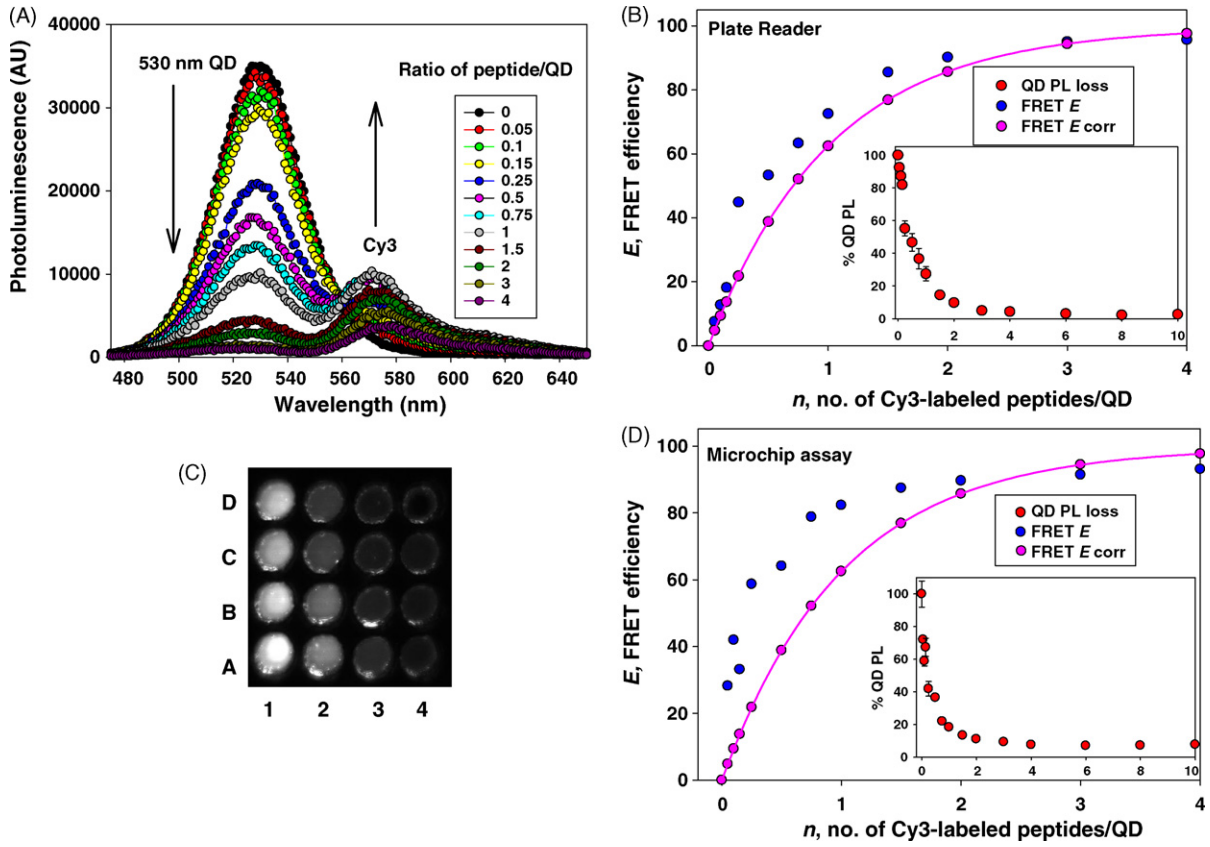

Fig. 3. QD-to-Cy3-peptide FRET efficiency. (A) PL spectra resulting from assembling an increasing number of Cy3-peptides per 530 nm QD-DHLA–PEG_{600}, taken using the Tecan Plate Reader and a 96-well assay plate (only ratios 0–4 plotted). (B) Corresponding FRET efficiency (blue) and the corrected FRET efficiency (pink) from (A) as a function of Cy3-peptide:QD ratio. Inset, QD PL quenching from (A) as a percentage (red). (C) EL-CCD image of 16-well sample chip loaded with samples consisting of an increasing ratio of Cy3-peptides per 530 nm QD-DHLA–PEG_{600}. Samples were loaded consecutively with increasing ratios from 1A (ratio 0) to 1D followed by columns 2–4, with 4C being the highest ratio (10) and 4D a buffer control (no QD or Cy3-peptide). (D) Corresponding FRET efficiency (blue) and corrected FRET efficiency (pink) from (C), both as a function of Cy3-peptide:QD ratio. Inset, QD PL quenching from (C) as a percentage of initial value (red) and calculated using ImageJ. (For interpretation of the references to colour in this figure legend, the reader is referred to the web version of the article.)

collected on the plate reader, compare Fig. 3B and D. The discrepancy may be attributed to difficulties in estimating *E* when using molar ratios smaller than one. For the microchip, however, the experimental *E* may be slightly overestimated since the emission filter used (with a 515–555 nm bandpass range) discards a fraction of the QD PL spectrum on both ends.

Regardless, analysis of the FRET *E* data (using a QD quantum yield of 20% and a R_0 value of 5.3 nm for this QD-dye pair) yielded an average center-to-center separation distance of 4.5 nm for the Plate Reader and 4.1 nm for the microchip data. These values clearly reflect a compact QD-peptide-dye configuration and very close proximity between dot surface and dye. This may be further facilitated by the peptide structure; the latter includes several proline residues in its sequence, which promote bending and an overall conformation that brings the dye closer to the QD surface [43]. Our measured FRET efficiencies contrast with those reported by Shi et al. [44] where 48 dye-labeled peptides were used to achieve comparable rates of FRET. The necessity for this high ratio in their conjugate can be partially attributed to the low quantum yield of their QDs after surface capping with the peptides.

3.3. Trypsin proteolytic assays

Confident that the microchip format could provide reasonable information on FRET efficiency and its dependence on the dye-peptide-to-QD ratio, we proceeded to perform monitoring of trypsin proteolytic activity. Trypsin cleaves peptidyl sequences on the C-terminal side of lysine (*K*) and arginine (*R*) amino acid residues and the peptide substrate sequence used in this study is designed to express three potential cleavage sites, two following arginine residues and one following lysine. We chose to utilize this enzyme for a comparison of the two analytical platforms as trypsin is well characterized, readily available and widely applied.

In choosing the peptide-QD substrate ratio for assaying with the enzyme, we utilize the above FRET efficiency data as a calibration curve where selection of dye-to-QD ratio satisfies two important criteria: (1) high initial FRET efficiency, followed by (2) a large change in the measured FRET efficiency upon interaction with the target enzyme, which would result in a broad dynamic range of accessible changes in FRET correlating to changing enzymatic velocity. We thus chose to utilize an average ratio of two labeled peptides per QD. The QD-bioconjugates were allowed to self-assemble for 30 min prior to use and then exposed to the indicated increasing concentrations of trypsin for short 5–10 min assay times. This format allows access to a wide range of enzyme concentrations and spans the range from near zero activity to maximum velocity while allowing us to visualize the initial rates at each point. The resulting CCD image taken from the microchip trypsin assay is shown in Fig. 4A. Clearly as the concentration of trypsin increases so too does the QD PL recovery, resulting in larger fluorescence intensities collected on the CCD image. This is a direct result of the peptide cleavage and reduction of FRET-induced quenching, due to trypsin protease activity. The normalized QD PL recovery for assay solutions measured with both the Tecan Plate Reader and the

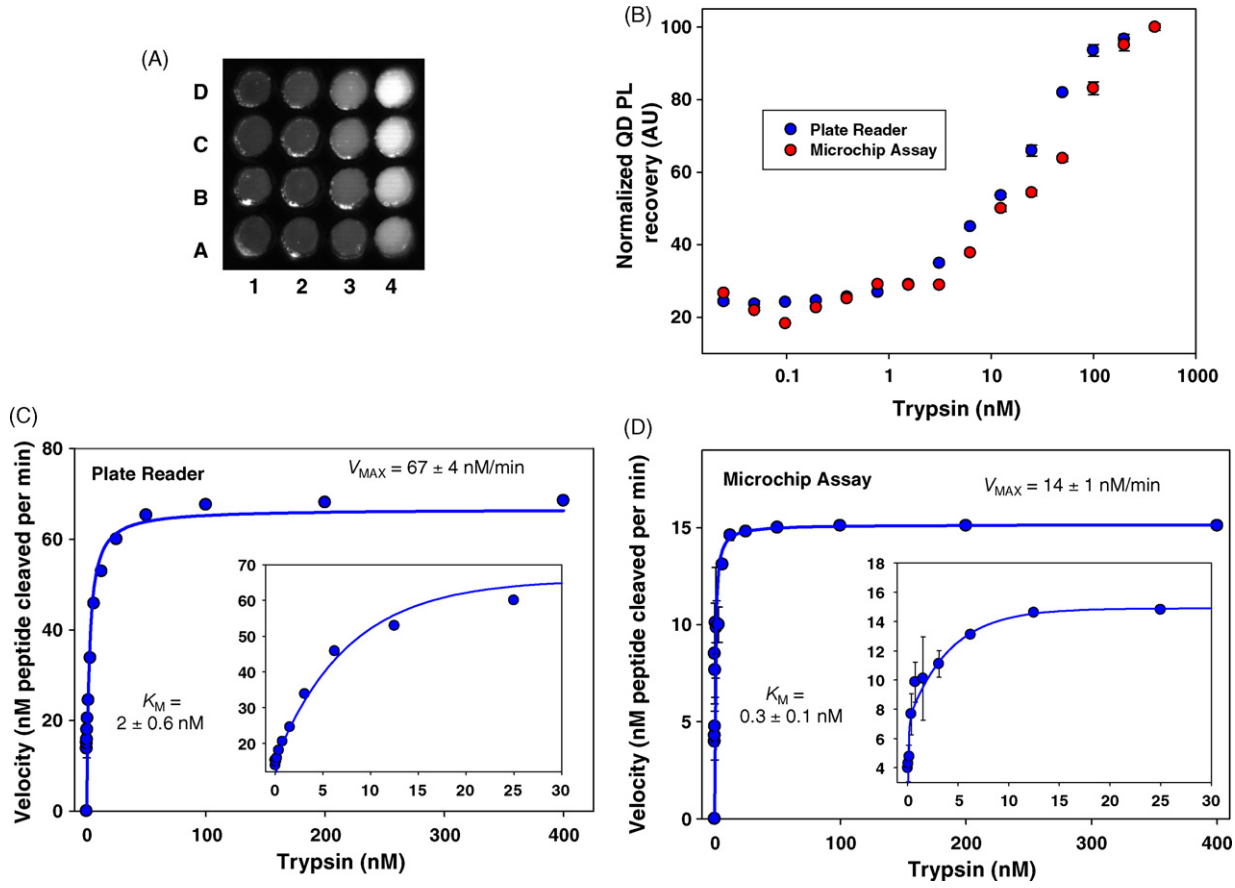

Fig. 4. QD trypsin assay. (A) EL-CCD image of 16-well sample chip loaded with the substrates. Samples were loaded consecutively with increasing concentrations of trypsin from 1A (0 nM trypsin) to 1D followed by columns 2–4, with 4D containing the highest concentration of trypsin, and each well containing the same amount of Cy3-peptide-QD bioconjugate. (B) Plot of normalized QD PL recovery due to protease activity versus the concentration of trypsin, as measured at 530 nm with the Tecan Plate Reader (blue circles) and from the microchip assay EL-CCD image in A (red circles). (C) and (D) are the trypsin activity plots derived using the data taken from the plate reader and the microchip assay, respectively. Estimated K_M and V_{max} values are indicated for each assay. Error bars represent standard deviations. Inset of each shows an expanded view of the velocities at the initial concentrations of enzyme used for each assay format. (For interpretation of the references to colour in this figure legend, the reader is referred to the web version of the article.)

microchip platform are shown in Fig. 4B. The data collated from the two systems show good agreement, with a limit of detection (LOD) of 6.2 nM trypsin (equivalent to 0.14 μg/mL). This 0.14 μg/mL trypsin LOD value, obtained after a 10 min incubation, is almost a 90-fold improvement over the 12.3 μg/mL detected by Grant and coworkers using a dual-organic fluorophore FRET peptide substrate immobilized on silica nanobeads and comparable to Shi et al., who obtained 0.1 μg/mL using peptide-QD FRET substrates and a 2 h incubation time [25,44].

The plots shown in Fig. 4C and D show the data converted into units of enzymatic velocity for the plate reader and the microchip, respectively. The resulting kinetic parameters including the Michaelis constant K_M, the maximal velocity V_{max}, the turnover number k_{cat} and the k_{cat}/K_M ratio are summarized in Table 1. There is a good overall agreement between the data extracted from both systems, with the microchip yielding a slightly higher-affinity K_M value. In comparison, the K_M = 34 μM derived by Grahn et al. using a DABCYL/EDANS dual-labeled FRET-based peptide substrate for trypsin suggests much lower affinity than that determined here [24]. This is most-likely a result of the presence of three potential cleavage sites within the peptidyl substrate sequence used in this study, contributing to the increased sensitivity by increasing the number of productive enzyme–substrate interactions.

Table 1
Kinetic parameters determined in this study

Method/conditions	K_M (nM)	V_{max} (nM min^{-1})	k_{cat}[a] (min^{-1})	k_{cat}/K_M (M^{-1} min^{-1})
Plate Reader				
Trypsin	2 ± 0.6	67 ± 4	0.167	8.35×10^7
EL-CCD microchip				
Trypsin	0.3 ± 0.1	14 ± 1	0.035	1.17×10^8
Trypsin + inhibitor[b]	20 ± 10[c]	9 ± 2	0.022	1.10×10^6

[a] $k_{cat} = V_{max}/[E]$ in excess substrate, where $[E]$ = 400 nM (at highest concentration).
[b] Ovomucoid (M_W 28 kDa) concentration used = 1200 nM; K_i = 18.2 nM.
[c] $K_M^{app} = K_M(1 + \{[I]/K_i\})$.

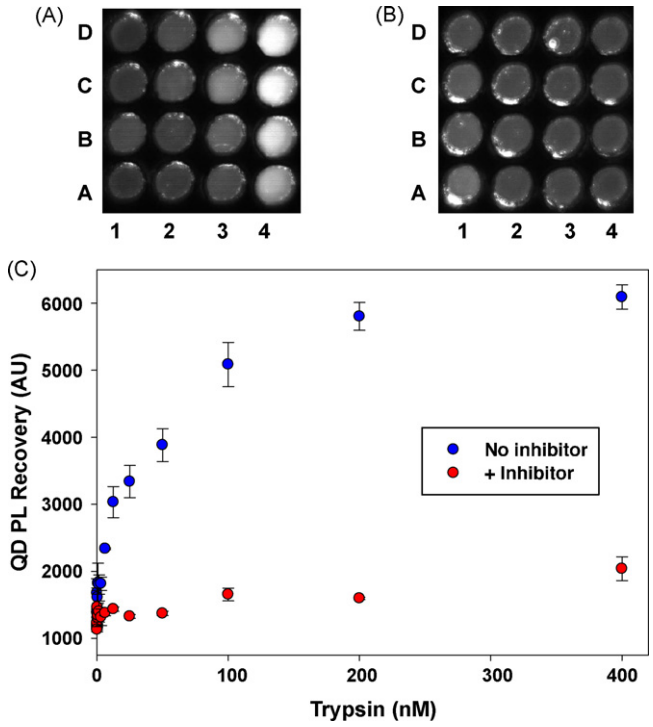

Fig. 5. QD trypsin inhibition assay. (A) and (B) are EL-CCD images of the 16-well sample chip loaded with the QD-peptide-Cy3 conjugates exposed to increasing concentrations of trypsin in the absence and presence of inhibitor, respectively. (C) Plot of QD PL recovery versus the concentration of trypsin in the absence (blue circles) and presence (red circles) of inhibitor, as measured from the EL-CCD images (A) and (B). The corresponding kinetic parameters are presented in Table 1. (For interpretation of the references to colour in this figure legend, the reader is referred to the web version of the article.)

3.4. EL-CCD microchip inhibition assay

To demonstrate the utility of this peptide-QD protease biosensor in an on-chip format, we assayed trypsin activity in the presence of the known specific inhibitor ovomucoid. Pre-assembled Cy3-peptide-QD bioconjugates were exposed to the various concentrations of trypsin in the absence or presence of 1.2 μM ovomucoid. In the absence of inhibitor, trypsin efficiently cleaves the peptide resulting in the expected PL increase of the QD (see Fig. 5A). This is clearly not the case in the presence of ovomucoid where almost no significant recovery of QD PL is seen, shown in Fig. 5B. Plots of the QD PL recovery measured from the CCD images are summarized in Fig. 5C and the corresponding kinetic parameters are listed in Table 1. Previous studies have demonstrated that ovomucoid functions as a competitive/reversible inhibitor of trypsin [45,46] and this is supported by the present set of data (see Table 1). The resulting dissociation constant K_i for ovomucoid calculated using a competitive inhibition model was found to be 18.2 nM, which is in excellent agreement with that determined by Lineweaver and Murray (16–18 nM) when ovomucoid inhibitor properties were first characterized more than 60 years ago [47].

4. Conclusions

By utilizing a peptide-QD substrate in a prototypic proteolytic assay we have been able to demonstrate several key QD-related attributes that may be important to their use in assays designed for microfabricated devices. In particular, the ability to control QD-acceptor FRET efficiency within the conjugate is key to optimizing an assay's performance and deriving quantitative results. The ability to use pH stable QDs capped with PEGylated ligands as demonstrated here will also allow access to a variety of assay pH's and conditions [33,34]. Beyond the protease assay demonstrated here, QDs may lend themselves to simplifying a variety of other detection needs using these devices including other enzymatic assays [48], immunoassays [13], or biosensing [49,50]. QDs may also allow access to multiplex FRET formats on microchips, where two or more assays are performed simultaneously. The latter is particularly challenging to achieve with conventional dyes in any format [10,14].

We also demonstrate the general parity of the results between the two QD-based assay formats and detection platforms even though the volumes utilized by the microchip were reduced by more than an order of magnitude. In this study the two detectors (EL-CCD platform and the Tecan Safire plate reader) showed good agreement with one another, with a similar LOD of 6.2 nM trypsin. The slight differences observed between the two instruments are likely a result of variations in measurement parameters; the plate reader used optimal excitation of 350 nm coupled with narrow excitation/emission bandwidths of 2.5 nm. The EL-CCD platform in comparison used an excitation of 480 nm with much broader bandwidths of between 20 and 40 nm, which may have contributed to the slight variations observed from donor–acceptor cross-talk. Although the microchip format may not be appropriate for extremely sensitive FRET studies, the simple design and nature of the EL-CCD platform, coupled to simpler monitoring when using QDs, makes it particularly suited to performing high-throughput low-sample volume screening not only of proteases and inhibitors but to a variety of other enzymatic, immunological and sensing assays. The 16-well microchips used in this study were optimized for the dimensions of the EL strip and the Pentax lens used, however, we are currently investigating and optimizing alternative wide angle lenses coupled with larger EL strips which would allow us to expanded and accommodate more sample wells up to and including 96 within the same microchip dimensions (5.4 cm × 7 cm), as desired. Applications for this platform may include onsite screening of large numbers of food, water or other consumable/agricultural samples, screening medical/clinical markers for POC diagnosis and global health applications.

Acknowledgements

The authors acknowledge NRL, the Office of Naval Research, the Army Research Office/Defense Threat Reduction Agency, the Office of Public Health Emergency Preparedness (OPHEP) IAG 224-05-655 (to A. Rasooly) and FDA contract HHSF223200610765P for financial support.

Appendix A. Supplementary data

Supplementary data associated with this article can be found, in the online version, at doi:10.1016/j.snb.2008.07.026.

References

[1] P. Yager, T. Edwards, E. Fu, K. Helton, K. Nelson, M.R. Tam, B.H. Weigl, Microfluidic diagnostic technologies for global public health, Nature 442 (2006) 412–418.
[2] A.J. deMello, Control and detection of chemical reactions in microfluidic systems, Nature 442 (2006) 394–402.
[3] A. Janshoff, H.J. Galla, C. Steinem, Piezoelectric mass-sensing devices as biosensors—An alternative to optical biosensors? Angew. Chem. Int. Ed. 39 (2000) 4004–4032.
[4] C.D. Chin, V. Linder, S.K. Sia, Lab-on-a-chip devices for global health: Past studies and future opportunities, Lab Chip 7 (2007) 41–57.
[5] K.E. Sapsford, C. Bradburne, J.B. Detehanty, I.L. Medintz, Sensors for detecting biological agents, Mater. Today 11 (2008) 38–49.

[6] C.A. Emrich, I.L. Medintz, W.K. Chu, R.A. Mathies, Microfabricated two-dimensional electrophoresis device for differential protein expression profiling, Anal. Chem. 79 (2007) 7360–7366.
[7] W.D. Ristenpart, J. Wan, H.A. Stone, Enzymatic reactions in microfluidic devices: Michaelis–Menten kinetics, Anal. Chem. 80 (2008) 3270–3276.
[8] I. Medintz, H. Uyeda, E. Goldman, H. Mattoussi, Quantum dot bioconjugates for imaging, labeling and sensing, Nat. Mater. 4 (2005) 435–446.
[9] X. Michalet, F.F. Pinaud, L.A. Bentolila, J.M. Tsay, S. Doose, J.J. Li, G. Sundaresan, A.M. Wu, S.S. Gambhir, S. Weiss, Quantum dots for live cells, in vivo imaging, and diagnostics, Science 307 (2005) 538–544.
[10] K.E. Sapsford, L. Berti, I.L. Medintz, Materials for fluorescence resonance energy transfer: beyond traditional 'dye to dye' combinations, Angew. Chem. Int. Ed. 45 (2006) 4562–4588.
[11] A.R. Clapp, I.L. Medintz, H. Mattoussi, Förster resonance energy transfer investigations using quantum dot fluorophores, Chem. Phys. Chem. 7 (2005) 47–57.
[12] A.R. Clapp, I.L. Medintz, J.M. Mauro, B.R. Fisher, M.G. Bawendi, H. Mattoussi, Fluorescence resonance energy transfer between quantum dot donors and dye-labeled protein acceptors, J. Am. Chem. Soc. 126 (2004) 301–310.
[13] E.R. Goldman, A.R. Clapp, G.P. Anderson, H.T. Uyeda, J.M. Mauro, I.L. Medintz, H. Mattoussi, Multiplexed toxin analysis using four colors of quantum dot fluororeagents, Anal. Chem. 76 (2004) 684–688.
[14] A.R. Clapp, I.L. Medintz, H.T. Uyeda, B.R. Fisher, E.R. Goldman, M.G. Bawendi, H. Mattoussi, Quantum dot-based multiplexed fluorescence resonance energy transfer, J. Am. Chem. Soc. 127 (2005) 18212–18221.
[15] X.S. Puente, L.M. Sanchez, C.M. Overall, C. Lopez-Otin, Human and mouse proteases: A comparative genomic approach, Nat. Rev. Genet. 4 (2003) 544–558.
[16] P. Vihinen, R. Ala-Aho, V.M. Kahari, Matrix metalloproteinases as therapeutic targets in cancer, Curr. Cancer Drug. Targets 5 (2005) 203–220.
[17] R. Ala-Aho, V.M. Kahari, Collagenases in cancer, Biochimie 87 (2005) 273–286.
[18] I. Richard, The genetic and molecular bases of monogenic disorders affecting proteolytic systems, J. Med. Genet. 42 (2005) 529–539.
[19] Y.M. Wu, X.Y. Wang, X. Liu, Y.F. Wang, Data-mining approaches reveal hidden families of proteases in the genome of malaria parasite, Genome Res. 13 (2003) 601–616.
[20] F. Shao, P.M. Merritt, Z.Q. Bao, R.W. Innes, J.E. Dixon, A *Yersinia* effector and a pseudomonas avirulence protein define a family of cysteine proteases functioning in bacterial pathogenesis, Cell 109 (2002) 575–588.
[21] K. Anand, J. Ziebuhr, P. Wadhwani, J.R. Mesters, R. Hilgenfeld, Coronavirus main proteinase (3CL(pro)) structure: basis for design of anti-SARS drugs, Science 300 (2003) 1763–1767.
[22] J.J. Schmidt, R.G. Stafford, Fluorigenic substrates for the protease activities of botulinum neurotoxins, serotypes A, B, and F, Appl. Environ. Microbiol. 69 (2003) 297–303.
[23] M. Taliani, E. Bianchi, F. Narjes, M. Fossatelli, A. Urbani, C. Steinkuhler, R. DeFrancesco, A. Pessi, A continuous assay of hepatitis C virus protease based on resonance energy transfer depsipeptide substrates, Anal. Biochem. 240 (1996) 60–67.
[24] S. Grahn, D. Ullmann, H.D. Jakubke, Design and synthesis of fluorogenic trypsin peptide substrates based on resonance energy transfer, Anal. Biochem. 265 (1998) 225–231.
[25] S.A. Grant, C. Weilbaecher, D. Lichlyter, Development of a protease biosensor utilizing silica nanobeads, Sens. Actuators B-Chem. 121 (2007) 482–489.
[26] C. Eggeling, P. Kask, D. Winkler, S. Jager, Rapid analysis of Forster resonance energy transfer by two-color global fluorescence correlation spectroscopy: Trypsin proteinase reaction, Biophys. J. 89 (2005) 605–618.
[27] E.D. Matayoshi, G.T. Wang, G.A. Krafft, J. Erickson, Novel fluorogenic substrates for assaying retroviral proteases by resonance energy transfer, Science 247 (1990) 954–958.
[28] I.L. Medintz, A.R. Clapp, F.M. Brunel, T. Tiefenbrunn, H.T. Uyeda, E.L. Chang, J.R. Deschamps, P.E. Dawson, H. Mattoussi, Proteolytic activity monitored by fluorescence resonance energy transfer through quantum-dot-peptide conjugates, Nat. Mater. 5 (2006) 581–589.
[29] C.B. Murray, D.J. Norris, M.G. Bawendi, Synthesis and characterization of nearly monodisperse CdE (E = sulfur, selenium, tellurium) semiconductor nanocrystallites, J. Am. Chem. Soc. 115 (1993) 8706–8715.
[30] L. Qu, Z.A. Peng, X. Peng, Alternative routes toward high quality CdSe nanocrystals, Nano Lett. 1 (2001) 333–337.
[31] B.O. Dabbousi, J. Rodriguez-Viejo, F.V. Mikulec, J.R. Heine, H. Mattoussi, R. Ober, K.F. Jensen, M.G. Bawendi, (CdSe)ZnS core–shell quantum dots: synthesis and optical and structural characterization of a size series of highly luminescent materials, J. Phys. Chem. B. 101 (1997) 9463–9475.
[32] H. Mattoussi, J.M. Mauro, E.R. Goldman, G.P. Anderson, V.C. Sundar, F.V. Mikulec, M.G. Bawendi, Self-assembly of CdSe–ZnS quantum dot bioconjugates using an engineered recombinant protein, J. Am. Chem. Soc. 122 (2000) 12142–12150.
[33] H.T. Uyeda, I.L. Medintz, J.K. Jaiswal, S.M. Simon, H. Mattoussi, Synthesis of compact multidentate ligands to prepare stable hydrophilic quantum dot fluorophores, J. Am. Chem. Soc. 127 (2005) 3870–3878.
[34] K. Susumu, H.T. Uyeda, I.L. Medintz, T. Pons, J.B. Delehanty, H. Mattoussi, Enhancing the stability and biological functionalities of quantum dots via compact multifunctional ligands, J. Am. Chem. Soc. 129 (2007) 13987–13996.
[35] J.R. Lakowicz, Principles of Fluorescence Spectroscopy, Springer, New York, 2006.
[36] T. Pons, I.L. Medintz, X. Wang, D.S. English, H. Mattoussi, Solution-phase single quantum dot fluorescence resonant energy transfer sensing, J. Am. Chem. Soc. 128 (2006) 15324–15331.
[37] D.A. Harris, Spectrophotometric assays, IRL Press, Washington DC, 1987.
[38] M. Dixon, The determination of enzyme inhibitor constants, Biochem. J. 55 (1953) 170–171.
[39] A.C. Bowden, Fundamentals of Enzyme Kinetics, Portland Press Limited, London, 1995.
[40] I.H. Segel, Enzyme Kinetics: Behavior and Analysis of Rapid Equilibrium and Steady-State Enzyme Systems, Wiley-Interscience, Hoboken, NJ, 1993.
[41] K.E. Sapsford, T. Pons, I.L. Medintz, S. Higashiya, F.M. Brunel, P.E. Dawson, H. Mattoussi, Kinetics of metal-affinity driven self-assembly between proteins or peptides and CdSe–ZnS quantum dots, J. Phys. Chem. C 111 (2007) 11528–11538.
[42] K.E. Sapsford, S. Sun, J. Francis, S. Sharma, Y. Kostov, A. Rasooly, Using spatial electroluminescent excitation for measuring botulinum neurotoxin A activity, Biosensors and Bioelectronics (in press), doi:10.1016/j.bios.2008.06.018.
[43] M. Malesevic, Z. Majer, E. Vass, T. Huber, U. Strijowski, M. Hollosi, N. Sewald, Spectroscopic detection of pseudo-turns in homodetic cyclic penta- and hexapeptides comprising beta-homoproline, Int. J. Peptide Res. Ther. 12 (2006) 165–177.
[44] L. Shi, N. Rosenzweig, Z. Rosenzweig, Luminescent quantum dots fluorescence resonance energy transfer-based probes for enzymatic activity and enzyme Inhibitors, Anal. Chem. 79 (2007) 208–214.
[45] I. Van der Plancken, M. Van Remoortere, A. Van Loey, M.E. Hendrickx, Trypsin inhibition activity of heat-denatured ovomucoid: A kinetic study, Biotechnol. Prog. 20 (2004) 82–86.
[46] J.M. Zhou, C. Liu, C.L. Tsou, Kinetics of trypsin inhibition by its specific inhibitors, Biochemistry 28 (1989) 1070–1076.
[47] H. Lineweaver, C.W. Murray, Identification of the trypsin inhibitor of egg white with ovomucoid, J. Biol. Chem. 171 (1947) 565–581.
[48] C.J. Xu, B.G. Xing, H.H. Rao, A self-assembled quantum dot probe for detecting beta-lactamase activity, Biochem. Biophys. Res. Commun. 344 (2006) 931–935.
[49] E. Goldman, I. Medintz, J. Whitley, A. Hayhurst, A. Clapp, H. Uyeda, J. Deschamps, M. Lassman, H. Mattoussi, A hybrid quantum dot-antibody fragment fluorescence resonance energy transfer-based TNT sensor, J. Am. Chem. Soc. 127 (2005) 6744–6751.
[50] K.E. Sapsford, T. Pons, I.L. Medintz, H. Mattoussi, Biosensing with luminescent semiconductor quantum dots, Sensors 6 (2006) 925–953.

Biographies

Kim E. Sapsford studied chemistry at the University of East Anglia (UEA, Norwich, UK) and in 2001 received her PhD in analytical chemistry developing optical biosensors. In 2001 she moved to the Center for Bio/Molecular Science and Engineering at the US Naval Research Laboratory, where she worked (until 2007) on creating fluorescent-based biosensors using the Array Biosensor technology developed by Dr. Frances Ligler. Currently she is a Staff Fellow at the US Food and Drug Administration (FDA) in the Office of Science and Engineering Laboratories (OSEL), Division of Biology (DB). Her work involves assessing biotechnology concerning public health safety in particular future biosensing technologies.

Igor L Medintz studied chemistry and forensic science at John Jay College of Criminal Justice, City University of New York (CUNY). In 1998, he received his PhD in molecular biology under Prof. Corinne Michels of Queens College (also CUNY). He carried out postdoctoral research under Prof. Richard A. Mathies (UC Berkeley) on the development of FRET-based assays using microfabricated devices for genetic analysis. Since 2002 he has been at the Center for Bio/Molecular Science and Engineering at the US Naval Research Laboratory where he is working in collaboration with Dr. Hedi Mattoussi on creating biosensors with quantum dots.

Dorothy Farrell received her BS in physics from Brooklyn College, City University of New York and her PhD from Carnegie Mellon University under Prof. Sara Majetich. After working as a postdoctoral research associate in the Majetich Lab, she moved to University College London in 2004 on a Royal Society USA/Canada Research Fellowship for 2 years. She currently works with Hedi Mattoussi at the Naval Research Lab as part of the National Research Council Research Associate Program. Her research focuses on nanoparticle synthesis and characterization.

Steven Sun studied at the University of Maryland Baltimore County (UMBC) and received a BS in computer engineering in 2007. He continued his education at UMBC and is currently pursuing a MS in computer engineering with a focus in optics and chip design, and biosensors. In 2007 he began work as a research engineer at the US Food and Drug Administration (FDA) in the Office of Science and Engineering Laboratories (OSEL). His work involves biotechnology and applications of computer engineering in the biosensor field for public health safety.

Avraham Rasooly obtained a BSc in Agronomy from the Hebrew University Faculty of Agriculture in 1978, an MSc in Genetics from the Hebrew University Department of Genetics, in 1982 and a PhD from the Michigan State University Dept. of Crop & Soil Science in 1988 for research on microbial nitrogen fixation. From 1988 to 1990, he conducted postdoctoral research first at Michigan State University on the genetics of fungal lignin degradation, and then from 1990 to 1995 as a Research Assistant Professor/Senior Research Scientist in the Dept. of Molecular Pathogenesis, Skirball Institute NYU Medical Center and the Public Health Research Institute of New York working on microbial genetics, the regulation of plasmid replication and

S. aureus pathogenesis. Dr. Rasooly joined the Food and Drug Administration (FDA) as a Microbiologist in 1995, where he is developing microbial detection approaches for foodborne pathogens and their toxins using biosensors and DNA microarrays. Currently Dr. Rasooly holds a joint FDA Center for Devices and Radiological Health (CDRH) and National Cancer Institute (NCI) appointment, continuing his research on microbial detection at FDA and serving as a program director at the Cancer Diagnostics Program of NCI, where he oversees research on novel technologies of cancer diagnostics.

Hedi Mattoussi earned a PhD in condensed matter physics from the University of Pierre and Marie Curie (Paris VI) in 1987. He was a postdoctoral fellow at the Polymer Science and Engineering (University of Massachusetts Amherst) and a visiting scientist at the Center for Materials Science and Engineering at MIT. He has been working at the US Naval Research Laboratory since 1997. His activity at NRL focuses on the development of QDs and QD-bioconjugates and their use in developing biological assays and imaging of live cells.